



Estimates of density of mesopelagic fish in the Southern Ocean derived from bulk acoustic data collected by ships of opportunity

Pablo C. Escobar-Flores^{1,2} · Richard L. O'Driscoll² · John C. Montgomery¹ · Yoann Lacroix² · Stefan Jendersie³

Received: 9 April 2019 / Revised: 28 November 2019 / Accepted: 2 December 2019 / Published online: 7 December 2019
© Springer-Verlag GmbH Germany, part of Springer Nature 2019

Abstract

The demand for information on mid-trophic level (MTL) organisms in open-ocean marine ecosystems has led to initiatives to collect acoustic data opportunistically in different regions around the world. Although, bulk acoustic data can provide information on the distribution patterns and dynamics of MTL organisms, it is necessary to convert acoustic-derived indices into biologically relevant quantities for parameterising and validating ecosystem and trophic models. A 7-year time series of acoustic data collected by ships of opportunity (SOOP) in the New Zealand sector of the Southern Ocean, information on species' distribution derived from trawl samples collected in research voyages, and target strength (*TS*) estimates obtained using a resonance-scattering model and literature *TS*–length relationships, were used to obtain the first estimates of density of mesopelagic fish in this region. Estimates of mesopelagic fish density decreased from north to south reflecting changes in species composition and scattering properties across three latitudinal regions (Northern, Central and Southern). Density estimates ranged from 16.4–40.1 in the north to 4.4–13.4 g m⁻² in the south. Catches revealed that the Northern region was dominated by *Lampanyctodes hectoris* and *Protomyctophum* sp. (Myctophidae) and *Maurollicus australis* (Sternoptychidae); the Central and Southern regions were dominated by the myctophids *Electrona antarctica* and *Protomyctophum* sp. and the Antarctic krill, *Euphausia superba*. Information on species composition was the main source of uncertainty in the density estimates, highlighting the need for more biological sampling. This study demonstrates that it is possible to integrate acoustic data collected opportunistically with auxiliary information from research voyages and literature to provide estimates of mesopelagic fish biomass in remote areas.

Keywords Mesopelagic fish · Backscatter · Southern ocean · Target strength · Ships of opportunity · Bootstrapping

Introduction

A key component of the open-ocean marine ecosystems is the mid-trophic level (MTL), which plays crucial ecological and biochemical roles: facilitating energy transfer between primary consumers and higher trophic levels; and actively participating in carbon fluxes and oxygen consumption across different depths in the water column through diel vertical migration (DVM) (Kloser et al. 2009; Catul et al. 2011; Bianchi et al. 2013; Irigoien et al. 2014). In open-ocean ecosystems, the MTL community is diverse and consists of a range of micronektonic organisms, including fish, crustaceans, squids and gelatinous zooplankton, although mesopelagic fish, particularly the families Myctophidae and Gonostomatidae, have been consistently recognised as the most dominant (Gjøsaeter and Kawaguchi 1980; Brodeur and Yamamura 2005; Nelson 2006; Irigoien et al. 2014). While their critical role in the ecosystem have been

Electronic supplementary material The online version of this article (<https://doi.org/10.1007/s00300-019-02611-3>) contains supplementary material, which is available to authorized users.

✉ Pablo C. Escobar-Flores
pablo.escobar@niwa.co.nz

- ¹ School of Biological Sciences, University of Auckland, Thomas Building, Building 110, 3a Symonds Street, Auckland Central, Auckland 1010, New Zealand
- ² National Institute of Water and Atmospheric Research, 301 Evans Bay Parade, Hataitai, Wellington 6021, New Zealand
- ³ Antarctic Research Centre, Victoria University of Wellington, Level 5, Cotton Building, Gate 7, Kelburn Parade, Kelburn, Wellington 6012, New Zealand

emphasised, recent studies have stressed that there are still large uncertainties about the biomass and community composition (Irigoiien et al. 2014; Escobar-Flores et al. 2018a) of the MTL.

Because of the limitations of net sampling (particularly catchability issues due to their small size, swimming ability and soft bodies, e.g. Kaartvedt et al. 2012) fisheries acoustics (hereafter acoustics) has become the standard sampling method for studying mesopelagic fish in open-ocean pelagic marine ecosystems (Gjøsaeter and Kawaguchi 1980; Handegard et al. 2013). Acoustic-derived measurements provide information for ecological studies, and for parametrising and validating ecosystem and trophic models (Lehodey et al. 2010, 2015). Acoustic data provides horizontally and vertically intensive, continuous, unobtrusive and georeferenced information, and it is capable of covering broad scales while sampling across pelagic habitats in a relatively short time span. Echosounders are commonly found on fishing vessels, which can be used to cost-effectively collect acoustic data opportunistically for scientific purposes (Kloser et al. 2009). This has fuelled initiatives for acoustic data collection and for standardising post-processing or data grooming through international collaboration (e.g. the Integrated Marine Observing System (IMOS), the National Center for Environmental Information, and the Southern Ocean Network of Acoustics), producing a large amount of potentially valuable information for ecological and modelling studies.

Acoustic data collected opportunistically has been used traditionally to study ecological aspects of the MTL in remote areas based on acoustic energy (backscatter) (e.g. Escobar-Flores et al. 2013, 2018a). However, more biologically meaningful variables such as fish density from schools or layers can be achieved through the echo-integration technique, which is based on the linearity principle that backscatter is proportional to the density of organisms (Simmonds and MacLennan 2005). This principle can be applied under two assumptions: first, targets are stochastically distributed in the ensonified volume with respect to each other; and second, that between successive transmissions individual targets move so new measurements are generated stochastically (Simmonds and MacLennan 2005). Although this principle holds true for targets with alike acoustic properties, in large-scale surveys where fish community composition is unknown and likely to change spatially or in the presence of multi-species aggregations, it may not apply. Target strength (TS) is species-specific, and even changes between individuals of the same species, particularly for myctophids, which display a variety of swimbladder shapes, and age-related swimbladder content change and atrophy (Marshall 1960; Davison 2011). Though acoustics has been used for estimating the abundance of MTL organisms (e.g. Gjøsaeter and Kawaguchi 1980; Irigoien et al. 2014), resonance scattering by siphonophores and small mesopelagic fish can obscure

the conversion and interpretation of acoustic energy as density (e.g. Davison et al. 2015a).

Previous estimates of mesopelagic fish density south and east of New Zealand (NZ) are limited to two studies: net-based estimates for the Sub-Antarctic and Antarctic regions of the South Pacific Ocean sector of the Southern Ocean (SO) combined, derived from an environmental conditions and fish density relationships (Gjøsaeter and Kawaguchi 1980); and, acoustics and net sampling abundance estimates for the epipelagic zone of four regions southeast and south of NZ (McClatchie and Dunford 2003). In this article, we advanced the use of acoustic indices derived from bulk data collected by ships of opportunity (SOOP) (see Escobar-Flores et al. 2018a, b), by producing more biologically meaningful estimates of mesopelagic fish density, which are the first for the NZ sector of the SO. Density estimates were obtained using: a 7-year time series of acoustic transects collected opportunistically between NZ and the northern area of the Ross Sea (RS); available information on species' composition and biological sampling collected in three research voyages; and target strengths from existing TS-length relationships and from a gas-bladder resonance-scattering model from the literature.

Materials and methods

Acoustic dataset

The acoustic dataset consisted of 28 transects collected by SOOP between NZ and the RS between November and March from 2008 to 2014, which is available through the IMOS portal (<https://portal.aodn.org.au/>). A detailed description of the acoustic data is available (Escobar-Flores et al. 2018a). Data collection took place during the austral summer because this is when the ice surrounding the Antarctic continent retreats, allowing access to the Antarctic toothfish (*Dissostichus mawsoni*) fishing grounds. Acoustic data was collected almost continuously by three toothfish fishing vessels (TFV) during their transits to and from toothfish grounds in the RS, and one research vessel (RV), Tangaroa, during research voyages in nearby waters of the Antarctic continent (Fig. 1). While all the TFVs (San Aotea II, San Aspiring and Janas) collected 38 kHz single frequency data, the RV Tangaroa collected multi-frequency data although only 38 kHz data were used here. Transceiver settings used during data collection were typically 2 ms pulse length and 2000 W power. Calibrations of the echosounders on board the TFV were carried out on a semi-regular basis by the National Institute of Water and Atmospheric Research (NIWA), following procedures as per Demer et al. (2015) using a 38.1 mm tungsten carbide sphere. Echosounders on the RV Tangaroa were calibrated at least annually.

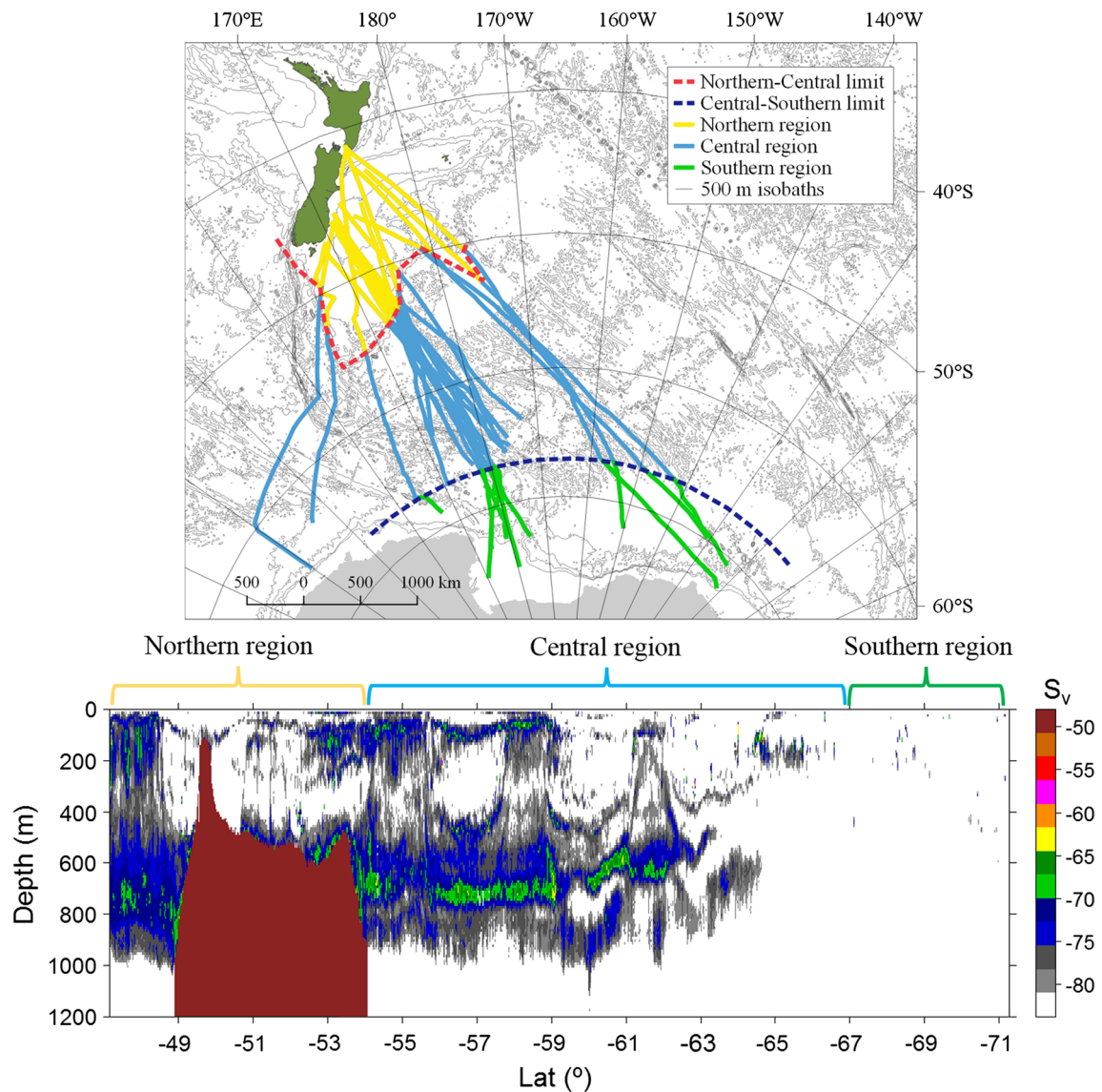


Fig. 1 Top panel shows the geographical location of acoustic transects which were split into three latitudinal regions between New Zealand (NZ) and the northern area of the Ross Sea (RS): Northern region (yellow, $n=27$), Central region (blue, $n=28$), and Southern region (green, $n=11$). Bottom panel shows the three regions along an acoustic echogram of transect collected by vessel ‘San Aotea II’

Grooming protocols for processing acoustic were based largely on the IMOS Bio-acoustic Ships of opportunity (BASOOP) sub-facility, using Matlab routines which operates through COM port objects to control Echoview (Echoview Software Pty Ltd 2013). Four noise filters were used for reducing the effect of common types of signal degradation when collecting acoustic data on board of SOOP, which have been described: impulsive noise, transient noise, background noise, and signal attenuation (Ryan et al. 2015). These filters were applied following (Ryan et al. 2015), with modifications per Escobar-Flores

between 9–16 February 2010 during its transit from the Southern Ocean (SO) (right) to NZ (left). Each pixel represents mean volume backscattering strength (S_v) in decibels (dB) echo-integrated in 1 km long and 10 m depth bins. Minimum echogram threshold: -84 dB for visualisation purposes only

(2017). In addition, Echoview’s background noise filter (De Robertis and Higginbottom 2007) implementation was also applied. For a complete description of the acoustic data processing, noise handling, and the performance of the grooming filters see Escobar-Flores (2017). Backscatter (in $m^2 m^{-2}$) was echo-integrated in 1 km horizontal and 10 m vertical (depth) bins, from 10 m from the surface down to 1200 m.

Acoustic transects are here referred to as group of acoustic raw files collected by a vessel during its transit from NZ to SO or from the SO to NZ, excluding data recorded in

toothfish fishing grounds due to commercial confidentiality (Table 1 and Fig. 1).

Each acoustic transect was split by latitude into three regions: Northern and Central regions were separated using 1500 m depth beyond the shelf break as the cut-off point (see Escobar-Flores et al. 2018a). The Southern region was defined from 67° S to the southernmost limit of the transect, which was variable and determined by the start of the fishing operation (see Fig. 1). Mean backscatter was calculated within the different latitudinal regions for each transect by averaging vertically summed backscatter at 1-km long bins.

Biological sampling

Biological information used for converting backscatter to mesopelagic fish density was collected on three research voyages carried out within the area of study by NIWA in 2008, 2011 and 2015 respectively (voyage codes: TAN0802, TAN1116 and TAN1502). A total of 51 trawls were used to characterise species' composition and were distributed between the three latitudinal regions as follows: Northern region 15 trawls from TAN1116; Central region 4 trawls from TAN0802 and 3 from TAN1502; and Southern region 13 trawls from TAN0802 and 6 from TAN1502 (Fig. 2). For detailed information on the sampling stations see Table S4 of the supplementary material in Escobar-Flores et al. (2018a). Sampling gear was a fine mesh mid-water trawl net with a 10 mm cod-end mesh and a headline height of 12–15 m, with a door spread of around 140–160 m. This mid-water gear is similar to the IYGPT (International Young Gadoid Pelagic Trawl), recommended by the Census of Antarctic Marine Life for sampling pelagic fish layers (www.caml.aq). Two types of tows were carried out: those used for acoustic mark identification (referred hereinafter as mark ID); and oblique (OB) tows. Mark ID trawls were carried out at day or night and had variable duration (10–40 min). For mark ID, the net was towed at the depth of the layer of interest at speeds of 3–4 knots. Most OB trawls were carried out at night time to characterise and estimate diversity, from 50 m above the sea-bed to the surface, at an ascent speed of 20 m per minute, and vessel speed of three knots.

Trawl catches were sorted and identified, when possible, to species or genus taxonomic level. From each trawl, biological subsamples of up to 100 individuals per species were

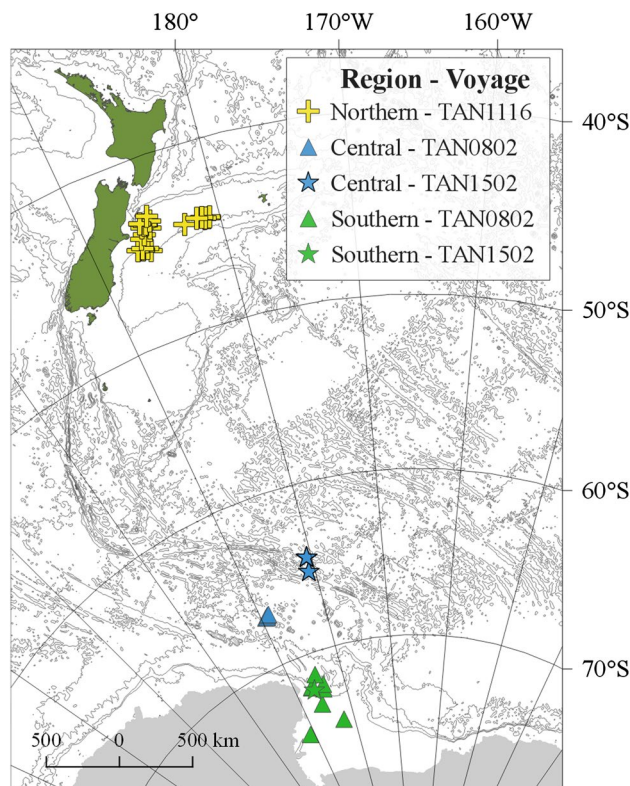


Fig. 2 Trawl locations from research voyages TAN0802 (triangles), TAN1116 (crosses) and TAN1502 (stars) grouped by regions: Northern (yellow), Central (blue) and Southern (green)

measured to the nearest 1 mm, and up to 20 individuals were weighted to the nearest 1 g. This information was used to establish species length–weight relationship and calculate the weight of organisms not weighed at sea [see Table S1 in the Electronic Supplementary Material (ESM) 1]. Species length and weight information were used to estimate target strength [TS in decibels (dB) re 1 m^{-1}] and backscatter to weight ratio (BWR in $\text{m}^2 \text{ kg}^{-1}$) respectively, for converting acoustic energy to biological density or abundance.

Species' composition from both trawl types was used to characterise each region (i.e. Northern, Central and Southern) for converting backscatter into density estimates. The dominant mesopelagic fish species by number and occurrence across trawls were used for this characterisation and to estimate density. Species having only an incidental

Table 1 Number of transects collected by ship of opportunity from 2008 until 2014 between New Zealand and the Ross Sea

Vessel name	No. of transects	2008	2009	2010	2011	2012	2013	2014
San Aotea II	11	1	–	2	2	2	2	2
San Aspiring	5	–	–	1	2	1	1	–
Janas	6	–	–	1	2	–	1	2
RV Tangaroa	6	2	–	2	–	–	2	–

occurrence in the catches and those poorly represented in the catches were excluded. To convert backscatter into density using the information on species composition drawn from the trawls, we have assumed that this is representative of each region and has remained constant over time.

Literature information of mesopelagic fish community composition in the area of study was used as additional guidance to inform the characterisation (e.g. McClatchie and Dunford 2003; Gauthier et al. 2014).

Target strength–length (TS–L) relationships

Target strength (the logarithm form of an individual’s backscattering cross-section, σ_{bs}), relates to length by the equation $TS = m\text{Log}(L) + b$, where L is the standard fish length obtained from the biological sampling size distribution, and m and b are the species-specific slope and intercept (Simmonds and MacLennan 2005). TS–L relationships from the literature for species collected in the biological sampling, or the closest taxonomic level, were used for estimating individual acoustic contribution. Organism body shape and size, and (for fish species) swimbladder presence/absence and composition (see Table S2 in ESM 1), were considered for assigning TS–L relationships to species with no published relationships. For each species, two TS–L relationships from the literature were used to produce a minimum and maximum TS, to account for the variability amongst the available estimates. We used the range between these estimates for uncertainty analysis.

Model-based target strength

To account for resonance from gas-filled swimbladder of fish in our density estimates, we used a resonance-scattering model to estimate the TS based on Love (1978), following a similar implementation as in Kloser et al. (2002) and Scoulding et al. (2015). The model relies on the computation of the TS of a fish as a function of frequency, environmental parameters and its physical characteristics (swimbladder + tissue). All constants used in this study are given in Table 2.

Here, we kept frequency f (in Hz), size of the fish L (in m) and depth d (in m) as variables. All other parameters in the model were fixed or calculated from one of these variables. The TS is defined by

$$TS = 10\log_{10}\sigma_{bs} \tag{1}$$

where σ_{bs} is the backscattering cross-section given by

$$\sigma_{bs} = \frac{\chi^2 a_{esr}^2}{((\omega_0/\omega)^2 - 1)^2 + \delta^2} D(\theta) \tag{2}$$

where a_{esr} is the equivalent spherical radius (a_{esr} in m), the coefficient χ represents the enhancement of the

Table 2 Resonance model parameters values for gas-filled swimbladders used in this study

Parameter	Symbol	Value	Units
Dampening factor	δ	0.14	–
Percentage of volume of fish occupied by the swimbladder	p_{swb}	0.1	%
Water density	ρ_w	1.026	kg L ⁻¹
Real part of fish-flesh rigidity	μ_r	1×10^6	N m ⁻²
Ratio of air specific heat	γ_a	1.4	–

backscattering amplitude due to elongation (as defined in Ye 1997), ω_0 is the resonant angular frequency (Hz) of the prolate spheroid, δ is the dampening factor, and $D(\theta)$ is a directivity term depending on fish orientation. $D(\theta)$ can be estimated based on the length of the fish L (m) and its angle of orientation θ as:

$$D(\theta) = \text{sinc}\left(\frac{kL}{4}\sin\theta\right) \tag{3}$$

We assumed $\theta=0$ (broadside incidence), giving a directivity of 1.

ω_0 can be estimated as

$$\omega_0^2 = \frac{C_e^2}{a_{esr}^2} \frac{3\gamma_a P + 4\mu_r}{\rho_w} \tag{4}$$

where C_e is the elongation factor as defined in Love (1978), γ_a is the ratio of the specific heat for air, μ_r is the real part of the rigidity of fish flesh, and ρ_w is the density of water (kg L⁻¹).

We calculated a_{esr} (in m) as in Proud et al. (2018), using the following approximation

$$a_{esr} = \left(\frac{3p_{swb}V_f}{4\pi}\right)^{\frac{1}{3}} \tag{5}$$

where p_{swb} is the percentage of the total volume of the fish used by the swimbladder using as reference values reported by Yasuma et al. (2010), and V_f is the total volume of the fish (L), V_f itself is approximated using the length of the fish L (m) and its aspect ratio α

$$V_f = \frac{1}{3} \left(\frac{\pi L^3}{2\alpha^2}\right) \tag{6}$$

To incorporate resonance of some species at depth, we defined a vertical distribution range $p(z)$ metres at day and night for each species based on available information in the literature and our biological sampling for each region (Northern, Central and Southern regions) (Table 3). The distribution was defined as a Gaussian-mixed model (see Eq. 7), to consider the range of depths that the species occupy at

Table 3 Vertical distribution range (defined as a layer) for each species at day and night for the Northern and Central region, and for the day distribution only for the Southern region, used to incorporate resonance in the target strength estimates

Species	Northern and Central region				Southern region	
	Day min. depth (m)	Day max. depth (m)	Night min. depth (m)	Night Max. depth (m)	Min. depth (m)	Max. depth (m)
<i>Diaphus</i> sp.	280	600	0	200	NA	NA
<i>Electrona carlsbergi</i>	280	1000	0	200	100	400
<i>Electrona antarctica</i>	200	1000	0	200	100	400
<i>Electrona paucirastra</i>	280	1000	0	200	100	400
<i>Krefflichthys anderssoni</i>	250	1000	0	250	0	400
<i>Lampanyctodes hectoris</i>	100	400	0	200	NA	NA
<i>Maurolicus australis</i>	100	300	0	200	NA	NA
<i>Photichthys argenteus</i>	280	600	0	200	NA	NA
<i>Protomyctophum</i> sp.	200	1000	200	1000	200	400
<i>Vinciguerria</i> sp.	280	600	0	200	NA	NA
<i>Cyclothone microdon</i>	300	1000	300	1000	200	400

NA not applicable (i.e. not present in the region)

day and night (for the Northern and Central region). Based on the vertical distribution of backscatter observed in the Southern region (see Fig. 1), we assumed a narrower vertical distribution range for this region, which did not change between day and night. The vertical distribution for a given species was defined as

$$p(z) = \frac{1}{n} \sum_{i=1}^n (\mu_i, \sigma_i^2), \quad (7)$$

where μ_i is the mean depth of the layer i , σ_i the standard deviation of the normal distribution for this layer, and n the number of the layer used for the species. σ_i was determined as

$$\sigma_i = \frac{1}{8} (z_{i,\max} - z_{i,\min}), \quad (8)$$

where $z_{i,\min}$ and $z_{i,\max}$ are the minimum and maximum depth for the layer i , respectively. Thus, we obtain the average backscattering cross-section, $\sigma_{\text{bs mean}}$, for each species incorporating possible resonance scattering for the species

$$\sigma_{\text{bs mean}} = \frac{\int_{z_0}^{z_1} p(z) \sigma_{\text{bs}}(z) dz}{\int_{z_0}^{z_1} p(z) dz} \quad (9)$$

Backscatter to weight ratio (BWR)

Backscatter to weight ratio (BWR) is the conversion factor to transform acoustic density (backscatter) to biological density of mesopelagic fish. For a particular trawl BWR in square metres per kilogram ($\text{m}^2 \text{kg}^{-1}$) was obtained as:

$$BWR = \frac{\sum_i^N 10^{(TS_i/10)}}{\frac{\sum_i^N w_i}{N}} \quad (10)$$

where N is the total number of fish biologically sampled in the trawl, w is the fish individual weight in kilograms (kg) of the i sampled fish, and TS_i is the TS in dB obtained for i fish length in cm.

Using bootstrapping to produce estimates of mesopelagic fish density and uncertainty

Estimates of mesopelagic fish density were obtained from the distributions of backscatter, species composition, and TS values derived from two scenarios for each region. In the first scenario, we used solely literature published $TS-L$ relationships, and in the second scenario, we allowed for resonance by including a resonance-scattering model. Confidence intervals were estimated by bootstrapping (Efron and Tibshirani 1993), which was considered the most appropriate method for incorporating uncertainty due to the relatively small sample sizes and varying forms of uncertainty. The statistical analyses used for estimating uncertainty (based on bootstrapping) was similar to those used in other acoustic studies (e.g. Rose et al. 2000; O'Driscoll 2004). Confidence intervals were obtained by resampling values (with replacement) from their respective distributions (see below) 1000 times.

For each region, we assumed that transects were our primary sampling unit and drew with replacement a sample size equal to the number of transects available on it to estimate their mean acoustic backscatter. This was repeated

1000 times to produce the backscatter bootstrap distribution. This distribution was used to draw backscatter values for the biological density estimates.

To incorporate the uncertainty of the species composition and TS estimates into the density estimates through the BWR bootstrap distribution in each region, a two-step process was followed. First, species composition uncertainty was included by resampling with replacement n trawls to produce a sample size equal to the number of trawls in a region (i.e. 25, 7 and 19 in northern, central, and southern regions respectively). Second, we estimated one lower and one upper BWR using the TS values obtained from the low and high $TS-L$ relationships for all the individuals of each species present in the catch for each trawl (first scenario). Under the second scenario the lower and upper BWR s were estimated in a similar fashion, but while there was one TS from the low and one high $TS-L$ relationships for fish without swimbladder, there was only one modelled TS for fish with gas-filled swimbladders. Following this approach, we produced two mean BWR s (mean from the lower and upper limit) for each trawl in both TS scenarios. A uniform distribution was assumed between the trawl lower and upper BWR boundaries (k_{lower} and k_{upper}), and a k proportion value (between 0 and 1) was randomly selected, representing the BWR value for the TS_{th} trawl. The k randomly selected BWR value at each n draw were then averaged (in the linear domain) over the number of trawls in a region, to complete one bootstrap sample. This was repeated 1000 times to generate the BWR bootstrap distributions. The bootstrap distributions of BWR under each scenario and the backscatter bootstrap distribution were used to estimate densities of mesopelagic fish and their associated confidence intervals.

To assess the relative contribution of each source of uncertainty in the density estimates (backscatter, species composition and $TS-L$ relationship uncertainty, assuming that the modelled TS is known without error) in each region, values from the other two sources were fixed at their median values, and 95% confidence intervals determined by bootstrapping only from the variable of interest. For example, in each region BWR had two uncertainty components: $TS-L$ relationships and species composition. To assess the uncertainty due to species composition, we assumed that the BWR of each station was known without error using the median, so trawls had different BWR that only reflected differences in their species composition. To assess the uncertainty due to $TS-L$ relationships, using the lower and the upper $TS-L$ relationships we estimated the median of lower and upper BWR s from all trawls (thus assuming that species composition is known without error), so that the BWR varied randomly following a uniform distribution between the BWR medians to reflect the uncertainty due to the $TS-L$ relationships. We followed this approach for both TS scenarios and compared the results obtained.

Results

Acoustic backscatter

A summary of mean backscatter by region is given in Table 4. Mean backscatter in the Northern and Central regions were more than one order of magnitude higher than backscatter in the Southern region. Histograms of the transect backscatter in each region are shown in Fig. 3.

Catch composition

As determined from the trawl catches the species diversity in the Northern region was dominated by fish, crustaceans and squids (61, 13 and 8 species, respectively). The overall diversity in the trawls from the Central and Southern regions not only decreased but was also dominated by the same three groups (Central region: 28 fish, 6 crustacean, and 9 squid species; Southern region: 23 fish, 4 crustacean, and 9 squid species). In this study, we only focussed on fish and crustaceans for density estimates (see “Discussion” section).

Detailed information on the catch and species composition by region available in Tables S4–S7 of the Supplementary Material in Escobar-Flores et al. (2018a). Excluding large non-mesopelagic fish species believed to have been caught only incidentally in the mid-water trawls (e.g. hoki, *Macruronus novaezelandiae*) as well as salps and jellyfish, the trawl catches of the Northern region were dominated by number by two myctophid species, *Lampanyctodes hectoris* and *Protomyctophum* sp. (19 and 3 trawls each), and the stomiiform *Maurollicus australis* (2 trawls). In the Central region, the myctophids *Electrona antarctica* and *Protomyctophum* sp. were the dominant species in 5 and 1 trawls each, and the Antarctic krill, *Euphausia superba*, dominated the remaining trawl. The trawl catches in Southern region were dominated by *E. superba* and *E. antarctica* (5 trawls each), followed by the Antarctic silverfish *Pleuragramma antarctica* (in three trawls), and the myctophid *Electrona carlsbergi* (in four trawls).

Averaged across trawls, the most commonly caught fish species by number or weight are shown in Table 5. By

Table 4 Transect sections per region including region mean acoustic backscatter (s_a) and standard deviation (SD), and mean number of bins per transect section

Region	No. of transect sections in region	Mean number of ~ 1 km bins	Mean s_a ($m^2 m^{-2}$)	SD
Northern	27	746	2.16×10^{-5}	2.27×10^{-5}
Central	28	1476	1.25×10^{-5}	1.17×10^{-5}
Southern	11	695	8.48×10^{-7}	3.36×10^{-7}

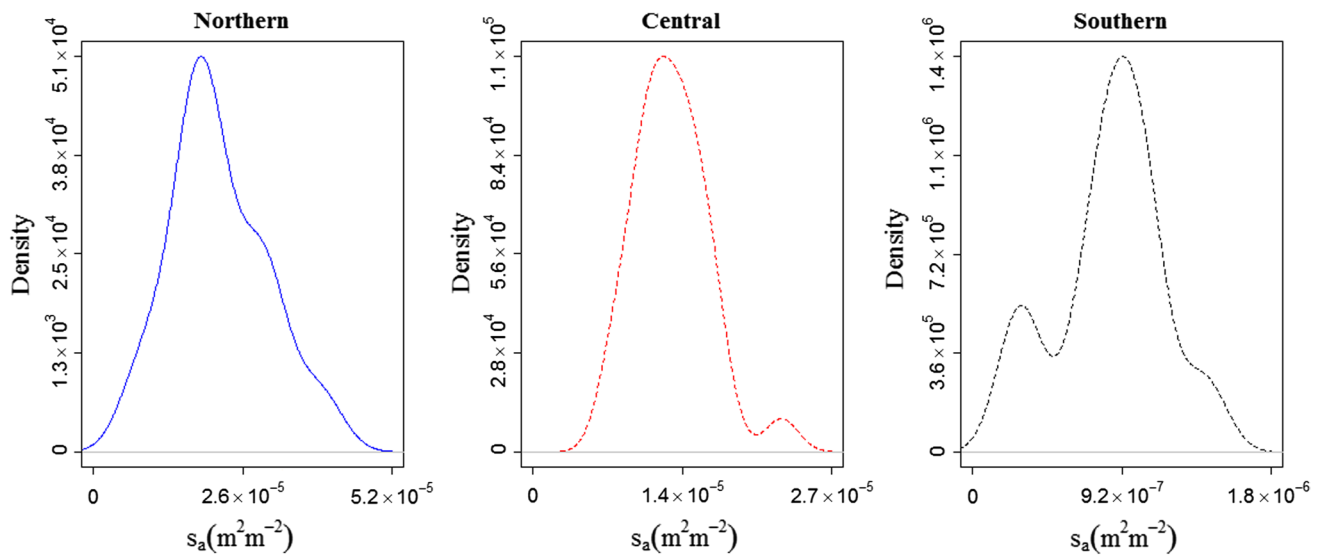


Fig. 3 Distribution of transects mean acoustic backscatter (s_a in $\text{m}^2 \text{m}^{-2}$) per region

number and weight, the myctophids *L. hectoris* dominated the fish fauna in the Northern region and *E. antarctica* in the Central region. Although, the notothenioid *P. antarctica* had the highest average contribution by weight in the Southern region, it was surpassed by number by *E. superba* and the crystal krill *Euphausia crystallorophias*, however, the latter was only present in three trawls. Although the myctophid *E. antarctica* was only the third most important species by number, and relative to other species had a lower weight contribution across trawls when present, it was the fish species most commonly caught (11 trawls) in the Southern region. Salps and jellyfish were also part of the catches (1 species caught in the Northern region and three in the Central and Southern), but these were not either identified to down to the level of species or considered for density.

Backscatter to weight ratio

The number of species sampled biologically (length or length and weight) varied between regions. Dominant species in each of the regions were used for biological density estimates. From the total number of species sampled in the Northern region, 14 out of 28 were included for *TS* estimates (and *BWR*), while in the Central and Southern regions 15 out of 28 and 18 out of 35 species were used, respectively.

TS–L relationships used for *TS* and *BWR* estimates in both scenarios are shown in Table 6. Where species-specific *TS–L* relationships were not available from the literature, relationships were based on species that were considered the best approximation to the species collected in the catches based on swimbladder (presence/absence), taxonomy and morphology (size and shape). Studies on *P. antarctica* have shown that the *TS–L* slope changes substantially across size

classes, leading to two different relationships with fish size (Azzali et al. 2010; O’Driscoll et al. 2011). This length split criterion for applying a *TS–L* relationship was used for all notothenioids. Lower and upper limits were based on the published range of *TS–L* relationships (Table 6).

Distribution of the *BWR* values per region used in both *TS* scenarios for density estimates are shown in Fig. 4. The range of the *BWR* values generated from both scenarios reflect the differences between the lower or upper *TS–L* relationship, since the average weight used for estimating both *BWR* for a trawl was the same. Under both scenarios the distribution of *BWR* are relatively similar, with some higher values standing out from the distribution drawn from the lower *TS* limit. There was a latitudinal trend in average *BWR*, with a decrease from north to south (Fig. 4).

Resonance scattering of mesopelagic fish

We considered a species to be contributing to backscatter at 38 kHz through resonance scattering, if the predicted resonance peak of a fish with a gas-filled swimbladder at a certain size was within ± 0.5 kHz from 38 kHz. The model predicted resonance for seven species of mesopelagic fish (Fig. 5). In the Northern region, resonance was predicted for individuals of the genera *Diaphus* and *Protomyctophum* as well as *E. carlsbergi*, *L. hectoris* and *M. australis*, for minimum and maximum fish sizes of 19 and 58 mm, equivalent spherical radius (a_{esr}) of 0.34 and 1.03 mm and resonance peak at depths 99 and 1000 m depth for *M. australis* and *E. carlsbergi*, respectively. In the Central region, four species were predicted to be resonant at 38 kHz, *E. carlsbergi*, *E. antarctica*, *Cyclothone microdon* and *Protomyctophum* sp. While relatively small individuals of *E. antarctica* (22 mm,

Table 5 Species used for density estimates in each region

Region	Order	Family	Species	Mean contribution to catch in number (%) across trawls when present \pm SD	Mean contribution to catch in weight (%) across trawls when present \pm SD	Occurrence	Mean length (cm) \pm SD	Mean weight (g) \pm SD	Total number
Northern	Myctophiformes	Myctophidae	<i>Lampasnyctodes hectoris</i>	70.8 \pm 29	39.2 \pm 31.8	22	5.2 \pm 5.6	0.9 \pm 0.3	129,764
Northern	Stomiiformes	Sternoptychidae	<i>Mauroliscus australis</i>	11.7 \pm 20.1	6.9 \pm 20.1	24	4.4 \pm 0.5	1.0 \pm 0.4	5835
Northern	Myctophiformes	Myctophidae	<i>Protomyctophum</i> sp.	8.2 \pm 15.2	2.3 \pm 3.4	20	5.5 \pm 1.3	2.4 \pm 1.5	528
Northern	Myctophiformes	Myctophidae	<i>Gymnoscopelus piabilis</i>	6.9 \pm 17.4	4.8 \pm 12.4	10	9.2 \pm 1.6	7.9 \pm 4.2	224
Northern	Myctophiformes	Myctophidae	<i>Lampanyctus</i> sp.	3.3 \pm 4.3	5.0 \pm 5.2	16	9.3 \pm 1.9	7.6 \pm 5	724
Northern	Myctophiformes	Myctophidae	<i>Electrona carlsbergi</i>	4.3 \pm 8.2	3.6 \pm 7.1	15	7.2 \pm 1	4.8 \pm 2	227
Northern	Myctophiformes	Myctophidae	<i>Symbolophorus boops</i>	1.7 \pm 1.5	5.0 \pm 5.6	14	8.7 \pm 1.3	10.1 \pm 4.9	2254
Northern	Myctophiformes	Myctophidae	<i>Diaphus</i> sp.	1.0 \pm 1.1	3.1 \pm 3.1	19	9.6 \pm 1.9	13.1 \pm 6	528
Central	Myctophiformes	Myctophidae	<i>Electrona antarctica</i>	38.2 \pm 22.7	18.7 \pm 0.8	6	6.7 \pm 1.3	4.7 \pm 3.2	615
Central	Argentiniiformes	Bathylagidae	<i>Bathylagus antarcticus</i>	12.5 \pm 1.5	18.7	3	12.3 \pm 3.2	23.5 \pm 18.7	116
Central	Myctophiformes	Myctophidae	<i>E. carlsbergi</i>	10.3 \pm 16.7	12.4 \pm 12.8	4	7.3 \pm 1.1	6.7 \pm 3.1	133
Central	Myctophiformes	Myctophidae	<i>Gymnoscopelus braueri</i>	9.2 \pm 5.7	7.5 \pm 1.4	4	21.7 \pm 1.5	99.3 \pm 18.9	113
Central	Stomiiformes	Gonostomatidae	<i>Cyclothone microdon</i>	8.5 \pm 5.4	3.7 \pm 3.1	4	5.9 \pm 0.8	0.8 \pm 0.2	105
Central	Myctophiformes	Myctophidae	<i>Protomyctophum</i> sp.	18.5 \pm 18.3	10.1 \pm 9.3	2	4.1 \pm 0.7	0.8 \pm 0.3	36
Central	Myctophiformes	Myctophidae	<i>Gymnoscopelus nicholsi</i>	5.8 \pm 3.5	13.8 \pm 4.8	6	14.9 \pm 0.9	32.9 \pm 5.8	84
Central	Aulopiiformes	Paralepididae	<i>Notolepis coatsi</i>	3.5 \pm 3.3	5 \pm 3.3	5	15.4 \pm 8	11.8 \pm 18.7	54
Central	Myctophiformes	Myctophidae	<i>Gymnoscopelus opisthopterus</i>	2 \pm 1.9	4.4 \pm 3.9	3	14.9 \pm 2.2	32.5 \pm 14	18
Central	Euphausiacea	Euphausiidae	<i>Euphausia superba</i>	21.3 \pm 50.3	11.0 \pm 18.1	6	4.4 \pm 1	0.6 \pm 0.4	901
Southern	Perciformes	Nototheniidae	<i>Pleuragramma antarctica</i>	51.4 \pm 47.5	44.4 \pm 51.8	7	13.2 \pm 3.7	22.9 \pm 19.3	26,475
Southern	Myctophiformes	Myctophidae	<i>E. carlsbergi</i>	37.0 \pm 32.5	23.2 \pm 16.6	7	7.9 \pm 1.1	7.4 \pm 4.5	311
Southern	Myctophiformes	Myctophidae	<i>E. antarctica</i>	21.4 \pm 10.6	8.4 \pm 7.2	11	7.4 \pm 1.6	6.4 \pm 4.1	477
Southern	Perciformes	Channichthyidae	<i>Neopagetopsis ionah</i> ^a	12.9 \pm 22.6	35.3 \pm 46.2	5	38.5 \pm 5.3	430.1 \pm 154.8	28
Southern	Argentiniiformes	Bathylagidae	<i>Bathylagus antarcticus</i>	15.9 \pm 14.8	18.7 \pm 15.3	9	12.2 \pm 3.9	22.1 \pm 21.1	238

Table 5 (continued)

Region	Order	Family	Species	Mean contribution to catch in number (%) across trawls when present \pm SD	Mean contribution to catch in weight (%) across trawls when present \pm SD	Occurrence	Mean length (cm) \pm SD	Mean weight (g) \pm SD	Total number
Southern	Stomiiformes	Gonostomidae	<i>Cyclothone microdon</i>	12.9 \pm 7.2	4.5 \pm 2.5	5	6.3 \pm 0.6	1.0 \pm 0.4	120
Southern	Myctophiformes	Myctophidae	<i>G. braueri</i>	11.8 \pm 9	10.7 \pm 5.4	5	22.9 \pm 2	134.3 \pm 8.7	109
Southern	Aulopiiformes	Paralepididae	<i>N. coatsi</i>	9.6 \pm 9.7	6.6 \pm 6.7	10	15.2 \pm 6.9	9.6 \pm 16.2	144
Southern	Myctophiformes	Myctophidae	<i>G. opisthopterus</i>	6.0 \pm 5.9	13.1 \pm 7.5	7	13.6 \pm 3.6	29.3 \pm 18.8	78
Southern	Myctophiformes	Myctophidae	<i>Gymnoscopelus bolini</i>	1.8 \pm 0.1	14.4 \pm 4.6	2	22.9 \pm 1.3	124.3 \pm 18.9	4
Southern	Myctophiformes	Myctophidae	<i>Gymnoscopelus hintonoides</i>	2.1 \pm 1.7	5.7 \pm 1.8	5	11.3 \pm 0.7	20 \pm 3.9	12
Southern	Myctophiformes	Myctophidae	<i>G. nicholsi</i>	5.1 \pm 2.9	8.1 \pm 7	9	14.9 \pm 1.4	33.9 \pm 4	62
Southern	Euphausiacea	Euphausiidae	<i>Euphausia superba</i>	64.1 \pm 31.6	25.6 \pm 36.7	6	4.6 \pm 0.6	0.7 \pm 0.3	82,273
Southern	Euphausiacea	Euphausiidae	<i>Euphausia crystallorophias</i>	53.1 \pm 65.6	30.7 \pm 34	2	3.1 \pm 0.4	0.1 \pm 0.1	2310

Only species that contributed on average by more than 2% to the total catch by number or weight across research trawls, and were present in at least two trawls were included (occurrence)

^aInfluenced by two trawls with 11 and 13 individuals of *N. ionah* over a total catch of 21 and 111 individuals, respectively. When these trawls were removed contribution dropped to <0.2%. This species was not included in density estimates

a_{esr} 0.39) were predicted to have a resonance peak at 136 m, the peak of larger individuals (58 mm, a_{esr} 1.03 mm) was predicted at the maximum vertical range (1000 m). Individuals of *C. microdon* of sizes 45 to 78 mm were resonant with resonance peaks over a broad vertical range (303–929 m) because of the small predicted a_{esr} sizes (0.57 to 0.99 mm) in comparison to other species. As in the Central region, *E. antarctica* and *C. microdon* were predicted to resonate in the Southern region, for fish sizes of 31 mm for *E. antarctica* (a_{esr} = 0.55 mm) and between 45 to 52 for *C. microdon* (a_{esr} from 0.57 to 0.66 mm) at depths between 303 and 400 m. These results show that resonance scattering occurs in all regions as a combination of changes in species' composition and fish sizes, with the potential for shaping spatial patterns of backscatter.

Estimates of biological density

Estimates of density obtained under both *TS* scenarios were reasonably similar and were within the same order of magnitude, however, they showed different spatial patterns (see Table 7). When *TS* were estimated using the

resonance-scattering mode (i.e. including resonance), mean mesopelagic fish density was highest in the Northern region and decreased south, which is consistent with the observed latitudinal patterns of backscatter between NZ and the northern area of the RS (see Table 4). Though the spatial pattern was the same, the differences between regions in terms of fish density were only subtle compared to the differences in backscatter (see Table 7). These results contrast with those obtained when using *TS* from the literature *TS*–*L* relationships not including resonance, where the highest densities of mesopelagic fish were found in the Central region. Under both scenarios, the lowest densities were in the Southern region (see Table 7).

The bootstrap distributions of backscatter, *BWR* and biological density, with 95% CI, are illustrated in Fig. 6. Biological density, backscatter and *BWR*, were all significantly higher in the Central region than in the Southern region. Backscatter and *BWR* were also significantly higher in the Northern than in the Southern region, but the difference in derived density estimates was not statistically significant between these regions (Fig. 6).

Table 6 Target strength (TS)–length (L) relationships available in the literature used for estimates of biological density

Group	Lower or upper TS	TS–L relationship based on	Applied for	TS–L relationship	TS–L source	Length range (mm)	References
Mycetophids with a gas-filled swim-bladder	Upper	<i>Diaphus theta</i>	<i>Electrona</i> spp., <i>Diaphus</i> sp., <i>Krefflichthys anderssoni</i> , <i>Protomyctophum</i> sp., <i>C. microdon</i> , <i>Vinciguerrria</i> sp. ^a	$TS = 11.8 \times \text{Log}_{10}(L) - 63.5$	Model (PSM)	26.9–77.4	Yasuma et al. (2003)
	Lower	<i>Ceratospinelus warmingii</i>		$TS = 26.3 \times \text{Log}_{10}(L) - 78.1$	Model (PSM)	33–83	Yasuma et al. (2010)
Mycetophids with atrophied, unformed or reversed swim-bladder	Upper	<i>Symbolophorus californiensis</i>	<i>Gymnoscopelus</i> spp., <i>S. boops</i> , <i>Lamparyctus</i> sp., <i>Nannobranchium achirus</i>	$TS = 20 \times \text{Log}_{10}(L) - 85.7$	Model (DCM)	85–108.4	Yasuma et al. (2003)
	Lower	<i>Diaphus chrysothyechus</i>		$TS = 30.5 \times \text{Log}_{10}(L) - 96.3$	Model (DCM)	62–100	Yasuma et al. (2010)
<i>L. hectoris</i> (Myctophidae)	Upper	<i>L. hectoris</i>		$TS = 20 \times \text{Log}_{10}(L) - 67.51$	In situ	41.6–65	Coetzee et al. (2006)
	Lower	<i>C. warmingii</i>		$TS = 26.3 \times \text{Log}_{10}(L) - 78.1$	Model (PSM)	33–83	Yasuma et al. (2010)
<i>M. australis</i> (Sternopychidae)	Upper	<i>M. australis</i>		$TS = 20 \times \text{Log}_{10}(L) - 66.36$	In situ	40–52	Coetzee et al. (2006)
	Lower	<i>Maurolicus japonicus</i>		$TS = 17.6 \times \text{Log}_{10}(L) - 67.4$	Model (PSM)	30.4–46.8	Fujino et al. (2009)
Fish without swim-bladder	Upper	<i>Scomber scombrus</i>	<i>B. antarcticus</i>	$TS = 20 \times \text{Log}_{10}(L) - 84.9$	Ex situ	310–350	Edwards et al. (1984)
	Lower	<i>Idiacanthus antrostomus</i>		$TS = 50.95 \times \text{Log}_{10}(L) - 133.80$	Model (FCM)	58–385	Davison (2011)
Nothotenids	Upper	<i>P. antarctica</i>	<i>P. antarctica</i> , <i>N. coatsi</i> , <i>Lepidonotothen kempi</i>	$TS = 57.85 \times \text{Log}_{10}(L) - 123.77$	In situ	13–70	Azzali et al. (2010)
	Lower			$TS = 36.83 \times \text{Log}_{10}(L) - 103.62$	Ex situ	110–202.5	Azzali et al. (2010)
Physoclists	Upper	<i>Argentina silus</i> (Great silver smelt)	<i>Photichthys argenteus</i>	$TS = 146.8 \times \text{Log}_{10}(L) - 216$	Model (ADSM)	< 111	O'Driscoll et al. (2011)
	Lower	<i>Mallotus villosus</i> (Cape-lin)		$TS = 18.7 \times \text{Log}_{10}(L) - 82.1$	Model (ADSM)	> 111	O'Driscoll et al. (2011)
Antarctic krill	Upper	Crustacean zooplankton and micronekton	<i>E. superba</i>	$TS = 20 \times \text{Log}_{10}(L) - 68$	In situ	250–500	Foote et al. (1986)
	Lower	<i>E. superba</i>		$TS = 21.1 \times \text{Log}_{10}(L) - 74.3$	In situ	90–150	Rose (1998)
Ice krill	Upper	Crustacean zooplankton and micronekton		$TS = 34.85 \times \text{Log}_{10}(L) - 132.44$	In situ	Broad range (unspecified)	Greene et al. (1991)
	Lower	<i>E. superba</i>		–	Model (SDWBA ^b)	20–50	Calise and Skaret (2011)
Antarctic krill	Upper	Crustacean zooplankton and micronekton	<i>E. crystallorophia</i>	$TS = 57 \times \text{Log}_{10}(L) - 177.4$	Ex situ	13–36	La et al. (2015)
	Lower	Crustacean zooplankton and micronekton		$TS = 34.85 \times \text{Log}_{10}(L) - 132.44$	In situ	Broad range (unspecified)	Greene et al. (1991)

PSM prolate-spheroid model, DCM deformed-cylinder model, FCM fluid cylinder model (Stanton 1988), ADSM anatomically detailed scattering model (Macaulay et al. 2002)

^a *Vinciguerrria* sp. (Stomiiform with gas-filled swimbladder) described as morphologically comparable to *M. australis* and *Benthosema* spp. (Ménard and Marchal 2003)

^c Stochastic distorted-wave born approximation model (Demer and Conti 2005) revised by Calise and Skaret (2011) parameterised using default vertical distribution orientation $N(1,4)$

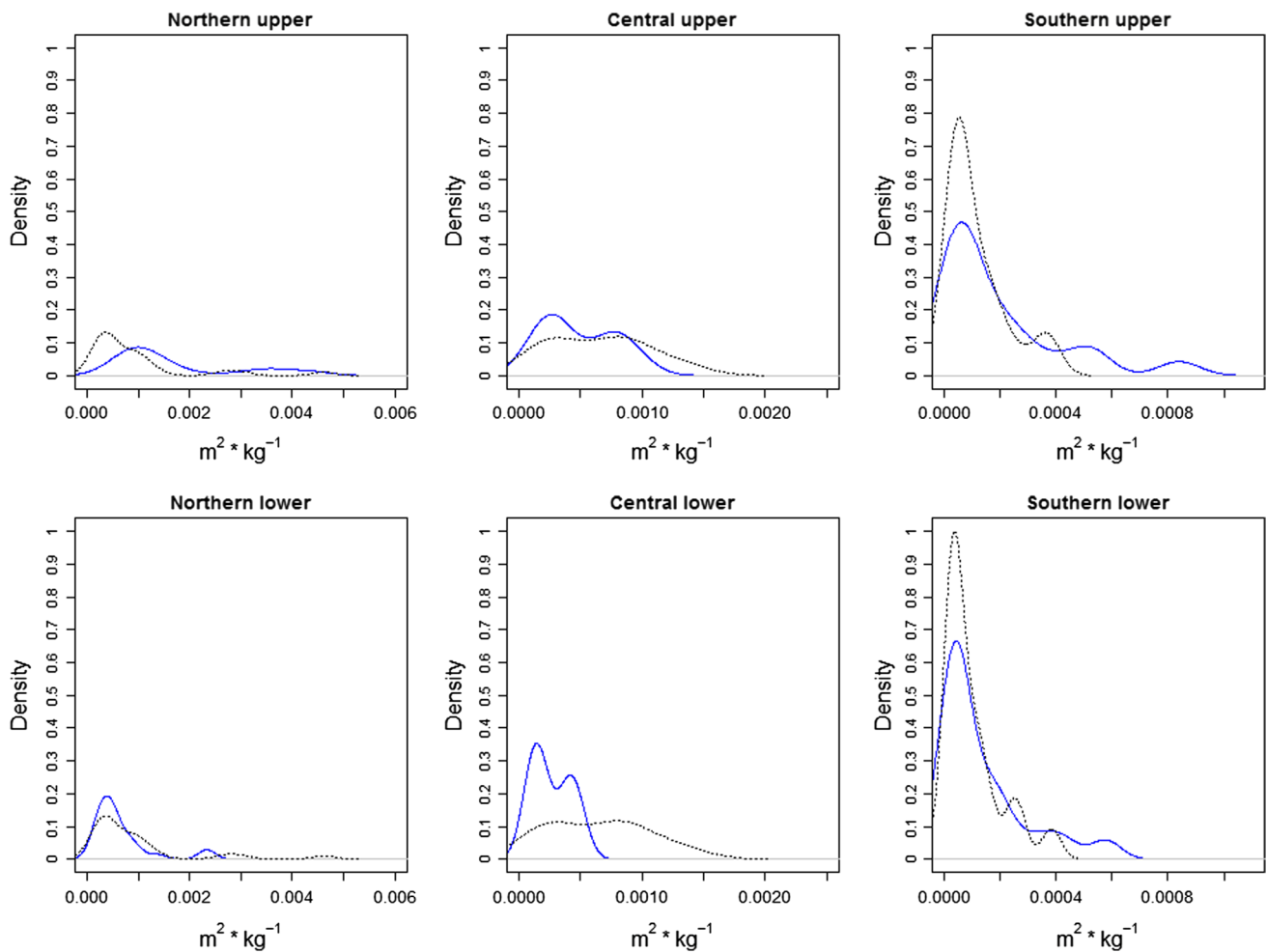


Fig. 4 Distribution of backscatter to weight ratio (BWR in $m^2 \text{ kg}^{-1}$) lower and upper limit for each region in both target strength scenarios (black dotted line including resonance, blue solid line not including resonance). Note the different scales used in the x -axes of the graphs

The estimates of density were more precise in the resonance scenario in the Northern and Central regions (see Table 8), because BWR obtained from modelled TS values were considered to be known without error. However, in the Southern region more precise estimates were obtained under the non-resonance scenario because the occurrence of fish without swimbladders was higher and because we restricted the depth range in scattering model to the top 400 m, which constrained resonance. In absence of resonance, the model produced lower TS values for fish with swimbladder with standard lengths < 10 cm compared to TS values obtained from TS – L relationships, explaining the lower density estimates for the Southern region under the resonance scenario (see example of TS for genus *Electrona* under both scenarios in the Southern region in Fig. 7).

Decomposing uncertainty

The main source of uncertainty in density estimates for all three regions was the species composition (see Table 8). The highest levels of uncertainty were found in the Central region, reflecting the low sampling in this area (7 trawls), and in the Northern region, which can be attributed to the higher species diversity in this area. Acoustic backscatter and TS were the second and third source of uncertainty in the estimates of density in all regions. The low uncertainty associated with TS is because the parameters used in the resonance-scattering model to estimate the TS parameters of fish with gas-filled swimbladders were defined as constants without error.

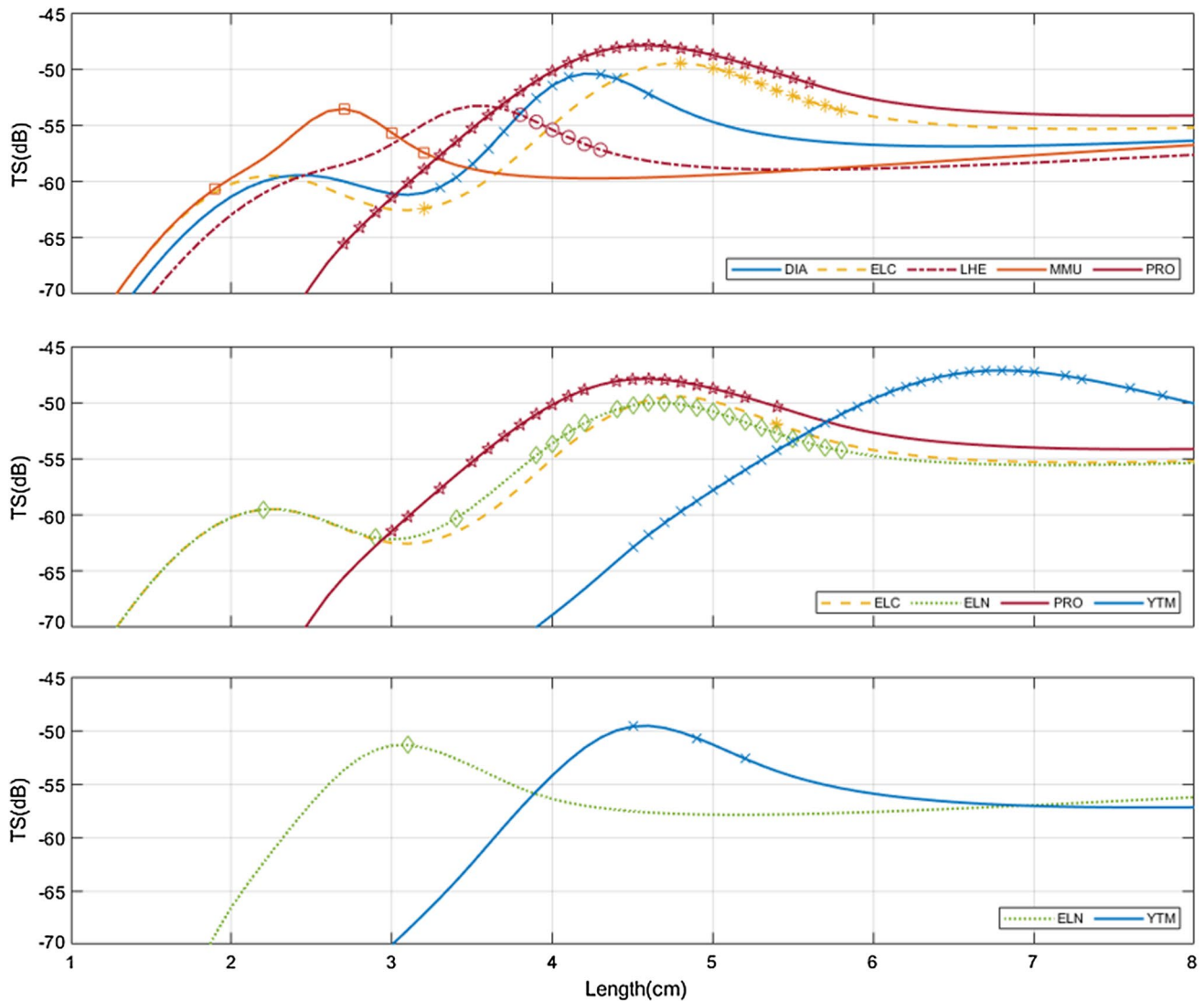


Fig. 5 Relationship between target strengths (TS) and fish size for the species considered as resonant at 38 kHz in each region (Northern, Central and Southern). TS were predicted using a resonance-scattering model based on (Love 1978) and the vertical distribution ranges for species presented in Table 3. Symbols show the predicted TS for the resonating fish of each species: Northern region: *DIA* *Diaphus* sp. (blue crosses), *MMU* *Maurollicus australis* (dark-red circles), *LHE*

Lampanyctodes hectoris (green diamonds), *ELC* *Electrona carlsbergi* (yellow asterisks), *PRO* *Protomyctophum* sp. (orange squares). Central region: *ELC* *Electrona carlsbergi* (blue cross), *PRO* *Protomyctophum* sp. (green diamonds), *ELN* *Electrona antarctica* (yellow asterisks), *YTM* *Cyclothone microdon* (dark-red circles). Southern region: *ELN* *E. antarctica* (blue cross), *YTM* *C. microdon* (yellow asterisks)

Discussion

A time series of bulk acoustic backscatter collected by SOOP, was combined with information on species' composition, and TS to produce the first estimates of density of mesopelagic fish in the NZ sector of the SO. Density estimates varied between three latitudinal regions, and although they matched the observed trends in acoustic backscatter, the differences of mesopelagic fish densities between regions were more subtle. This was due to changes in species' composition between regions, fish size, and resonance scattering. While estimated densities were plausible and comparable to

previous studies (see below), there was substantial uncertainty due mainly to limited biological data on species' composition. The differences in density between our two TS scenarios highlight the need for considering resonance scattering in the estimates of mesopelagic fish density. This requires more information on fish swimbladder morphology and ontogenic changes, if we aim to achieve reliable estimates of abundance.

Our estimates suggest that the density of mesopelagic fish for waters south and southeast of NZ may be higher than previously thought. For the southwest South Pacific Ocean Gjøsæter and Kawaguchi (1980) provided an estimate of

Table 7 Comparison of mesopelagic fish density estimates from our study using the backscatter to weight ratio values generated with the target strengths (*TS*) from the resonance-scattering model (resonance scenario) for fish with gas-filled swimbladders and *TS*-length relationships available in the literature for fish with atrophied or without swimbladder

Region	Depth	Method	Density (g m ⁻²)	Source
Northern region (NZ sector of the SO)	10–1200	Acoustics	16.4–40.1 (11.8–39.8)	This study
Central region (NZ sector of the SO)	10–1200	Acoustics	13–36.8 (21.1–63.9)	This study
Southern region (NZ sector of the SO)	10–1200	Acoustics	4.4–13.4 (2.8–9.4)	This study
Southwest South Pacific Ocean	200–1000	Analogy with similar areas	4.5	Gjøsaeter and Kawaguchi (1980)
East and southeast of NZ	16–200	Acoustics	0.3–18.2	McClatchie and Dunford (2003)
Southern California	175–525	Acoustics/trawl	25–37	Davison et al. (2015b)
Tasman Sea between Australia and NZ	0–600	Acoustics	16–29	Kloser et al. (2009)
Macquarie Island, SO	0–1000	Trawl (for myctophids only)	1.6	Flynn and Williams (2012)
Polar Frontal Zone north of South Georgia	Not available	Acoustics	5–15	Chindonova (1987)
Polar Frontal Zone north of South Georgia	Not available	Acoustics	3.8–6.5	Filin et al. (1990)
Polar Frontal Zone north of South Georgia	Not available	Acoustics	1.6–11.6	Kozlov et al. (1990)
Weddell Sea	0–1000	Trawl	3.3–4.4	Lancraft et al. (1989)
Northwest of South Georgia in the northern Scotia Sea	0–1000	Trawl	2.9	Collins et al. (2008)
Seasonal ice-edge to the PFZ in the Scotia Sea	0–1000	Trawl	2.2	Collins et al. (2012)
Eastern Ross Sea (RS) (> 68° S)	0–1000	Trawl	0.7	Donnelly et al. (2004)
Circumglobal expedition between 40° N and 40° S	200–1000	Acoustics	27–900 ^a	Irigoien et al. (2014)

Density estimates in brackets for the Northern, Central and Southern regions were obtained under the non-resonance scenario for comparison

^aUsing 25–75% quartiles of the *BWR* and an area of 222.3 million km² (Irigoien et al. 2014)

4.5 g m⁻² (see Table 7), which is at the lower end of the range of our estimates. Our estimates from the Northern region were comparable to those of McClatchie and Dunford (2003) from east and southeast of NZ, and those reported by Kloser et al. (2009) from acoustics across the Tasman Sea between Australia and NZ (see Table 7). Few studies from the region have reported higher density values, but Filin et al. (1990) estimated maximum mesopelagic fish densities between 70 and 100 g m⁻² and over, in areas of the Atlantic sector of the SO based on acoustics.

The 95% CI density that we estimated for the Southern region encompasses acoustic density estimates in the Polar Frontal Zone (PFZ) north of South Georgia (e.g. Kozlov et al. 1990), trawl estimates in the Weddell Sea (Lancraft et al. 1989), in the northwest of South Georgia in the northern Scotia Sea (Collins et al. 2008), and in the region between the seasonal ice-edge to the PFZ in the Scotia Sea (Collins et al. 2012) (see Table 7). Estimates of fish biomass reported by Donnelly et al. (2004) for the eastern RS (0.7 g m⁻²) using three types of sampling gear were below the lower end of our 95% CI, however, their trawls were restricted to latitudes greater than 68° S.

Including resonance scattering and including it in the mesopelagic fish density estimates led to lower densities

of mesopelagic fish in some areas (Central regions, around 40%), which is in agreement with some recent studies (e.g. Davison et al. 2015b; Proud et al. 2018).

Although our estimates of mesopelagic fish concurred with other regional studies in the SO, both our levels of backscatter in the pelagic zone (10 and 1200 m) and estimates of mesopelagic fish density in all three regions, were much lower than those provided by Irigoien et al. (2014) for mesopelagic fish biomass in temperate waters between 40° N and 40° S (see Table 7).

The main source of uncertainty in our density estimates was related to the species composition information provided by the biological sampling. This is unsurprising due to limited number and spatial coverage of available trawls for the NZ sector of the SO. The density estimates presented here also assumed that the catchability of the trawls was the same for all species, which is unlikely given the diversity of swimming capabilities, sizes, shapes and body compositions found in the MTL community. We acknowledge that by not including catchability, the accomplished species characterisation and results could have substantial bias (Heino et al. 2011; Gauthier et al. 2014; Davison et al. 2015b). However, by including biological information collected with two different sampling strategies (oblique and target tows) and

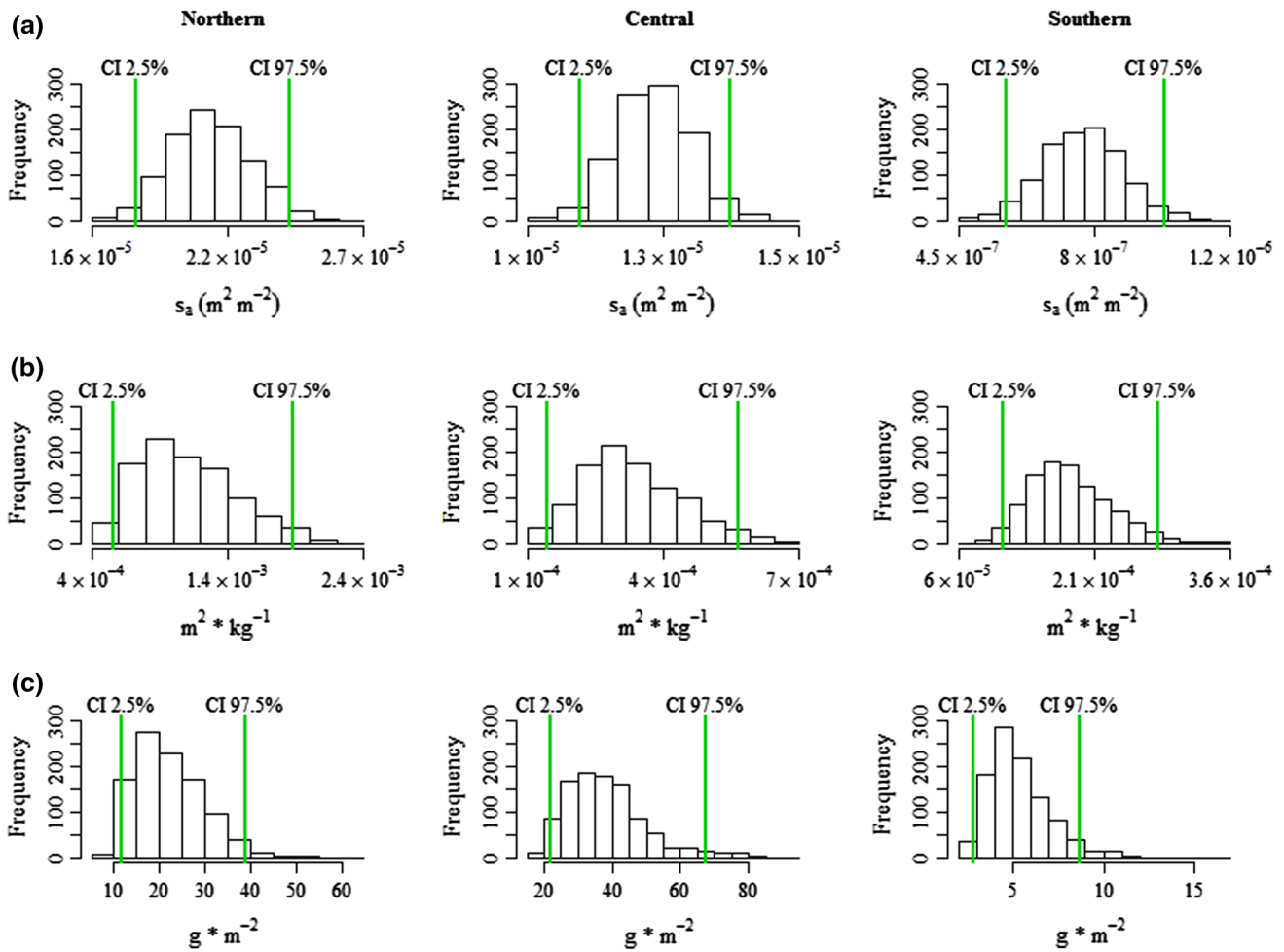


Fig. 6 Distribution of **a** acoustic backscatter (s_a in $m^2 m^{-2}$), **b** backscatter to weight ratio ($m^2 kg^{-1}$) and **c** density ($g m^{-2}$), based on transects backscatter, biological characterisation from three research voyages and *TS* values obtained from the resonance-scattering model,

generated for each region by bootstrapping. Estimates of density include three sources of uncertainty: s_a ; species composition; and *TS*-*L* (combined in $m^2 kg^{-1}$ backscatter to density conversion factor). Note the different scales used in the *x*-axes of the graphs

Table 8 Summary table with the 95% confidence intervals produced from bootstrapping when decomposing the three sources of uncertainty considered in the estimates of density of mesopelagic fish under the resonance scenario

Source of uncertainty	Region		
	Northern	Central	Southern
Acoustic backscatter	26–34.3	37.8–45.1	5.7–8.8
Species composition	22.2–42.7	24.7–90	4.4–14.4
Target strength	18.1–25.4	14.9–17.7	5.2–5.9

The 2.5th and 97.5th intervals of density estimates (in $g m^{-2}$) are shown when each of the sources of uncertainty was estimated independently in each region

some non-fish organisms (e.g. krill) in the species composition characterisation, some of the uncertainty around catchability was at least partially incorporated in the bootstrapped CIs presented. We also gave the same weighting to all trawls

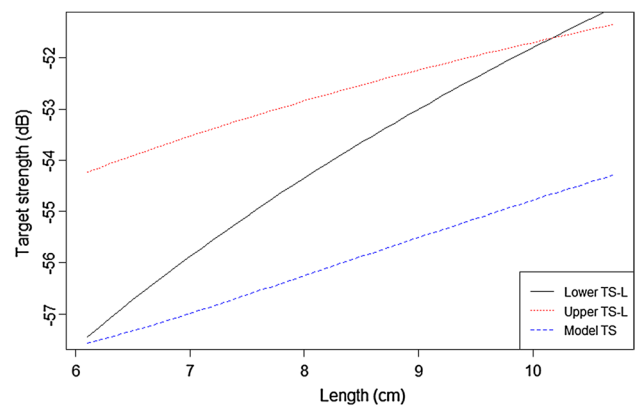


Fig. 7 Target strength (*TS*) obtained for individuals of the genus *Electrona* ($n=430$) collected in the Southern region using the lengths from the biological sampling, the lower and upper *TS*-*L* relationships (see Table 6) and the resonance-scattering model in absence of resonance

regardless the size of their catches, which could bias the length information used to estimate TS , however, we believe that this bias is relatively small compared to other sources of uncertainty included in the analyses. To reduce the uncertainty around species composition we need to increase the sampling effort and spatial coverage, use trawl nets of different mesh size and complement various sampling gears (e.g. net plus optics).

Although we incorporated resonance scattering in our density estimates, bias in sampling towards species of larger sizes, might have contributed to underrepresenting the abundance of the small fish responsible for resonant scattering. Conversely, in our resonance-scattering model we used a relatively small fixed percentage of volume of fish occupied by the swimbladder (0.1%). Although this value is within the range of direct measurements from mesopelagic fish swimbladder morphology (0.01–2.3%, Yasuma et al. 2010), we did not consider sensitivity to this or the other swimbladder model parameters. Potential resonance scattering of mesopelagic fish needs to be studied further in the SO, with emphasis on comprehensive biological and acoustical sampling, modelling of the scattering properties of mesopelagic fish, and on the ground-truthing of TS predictions from resonance-scattering models. Sensitivity analyses of modelling studies have identified that morphometric parameters such as the swimbladder volume and aspect ratio of the fish body are the main factors driving uncertainty in abundance estimates of mesopelagic fish (Proud et al. 2018), so species-specific measurements of these parameters are required. The lack of information on acoustic properties of mesopelagic fish is a common case, with only a few communities characterised acoustically, e.g. southern California current system (Davison et al. 2015b) and temperate zones of the Northwest Pacific (Yasuma et al. 2006, 2010; Sawada et al. 2011).

To date there is no TS – L relationship for any species in the region (McClatchie and Dunford 2003). Modelling has been commonly used to establish linear relationships between TS – L (e.g. Yasuma et al. 2003; Davison 2011), but resonance and ontogenic changes of the swimbladder may hinder their use for gas-bladdered species across a wide size and depth range (Davison 2011; Davison et al. 2015b; Scouling et al. 2015). For example, Dornan et al. (2019) reported an apparent loss of gas in swimbladders of *E. antarctica* for sizes > 5.1 cm length for fish collected in the Scotia Sea.

Acoustic backscatter showed a large-scale latitudinal pattern, with a statistically significant decrease from north to south in the NZ sector of the SO (Escobar-Flores et al. 2018a). Mean backscatter levels in the Northern region were more than 50% higher than in the Central region, and the levels of both these regions were more than one order of magnitude higher than in the Southern region (see Table 4). Density estimates did not show the same latitudinal degree

of change; estimated levels of density were higher in the Northern and lower in the Southern region, but the magnitude of the decrease was much less than that observed for backscatter.

Inconsistencies between backscatter and estimates of mesopelagic fish density were driven by the differences in the species composition and the acoustic properties of the species in each region. Information on species composition in our study was drawn from research voyages undertaken in different years, but the characterisation of the mesopelagic fish communities in the three regions was in agreement with previous regional studies, and also captured described changes in species composition with latitude in the SO (McGinnis 1982; McClatchie and Dunford 2003). Although the number of trawls used for abundance estimates in this study was small, there was a marked contrast in composition and species dominance between latitudinal regions: the northern region was dominated by *L. hectoris*; and the central and southern region were dominated by *E. antarctica* and *P. antarctica*, respectively. In addition, each region had at least one ‘endemic’ species which was not present elsewhere (e.g. *L. hectoris* only present in the Northern region and *P. antarctica* only present in the Southern region).

The species composition in the Northern region resembled that of an earlier study by Robertson et al. (1978), with myctophids (*L. hectoris*, *Symbolophorus boops*, *Gymnoscopelus* spp., *Lampanyctus* spp. and *Protomyctophum* sp.) and the sternoptychid *M. australis* the most abundant fish species. *L. hectoris* and *M. australis* have been described consistently as the most common and dominant over the Chatham Rise and Bounty Trough (east of NZ) (Robertson et al. 1978; McClatchie and Dunford 2003; Gauthier et al. 2014). These two species have gas-filled swimbladders (Marshall 1960), which makes them strong scatterers. This is because gas-filled swimbladders can account for around 90–95% of the acoustic response of a fish (Foote 1980; Davison 2011). In addition, many of these Northern swimbladder species can produce resonance scattering at 38 kHz. Consequently, BWR values in this region were high, leading to lower estimates of density since these species show a high contribution in terms of backscatter for relatively low weight.

The Central and Southern regions had lower BWR levels due to the higher occurrence of species without swimbladder (e.g. *P. antarctica*), species whose swimbladder regress with age (e.g. genus *Gymnoscopelus*) (Dornan et al. 2019), and euphausiids (e.g. *E. superba*). Many of the strong scattering species found in the Northern region are absent further south. Only one species of the genus *Electrona*, collected in the Northern region was found in the southern two regions. A wide latitudinal distribution range has previously been reported for *E. carlsbergi* (McGinnis 1982; Hulley 1990). Likewise, the incidence of species capable of resonating at

38 kHz in the Central and Southern regions was restricted to four and two species, respectively.

Although the species composition information collected in our trawls agreed with the extensive literature (e.g. Gjøsaeter and Kawaguchi 1980; Brodeur and Yamamura 2005) in suggesting that myctophids dominate the mesopelagic fish community, we acknowledge that backscatter could contain nektonic and planktonic organisms with different acoustic properties that were not considered as part of this analysis. Some trawls were dominated by tunicates or gelatinous zooplankton (e.g. salps and jellyfish). These groups can also scatter sound at 38 kHz (e.g. Wiebe et al. 2010) and so contribute to observed backscatter, although their overall contribution at 38 kHz frequency was assumed to be low (but see Brierley et al. 2001). Another potential bias can be caused by the presence of gas-bearing gelatinous organisms (e.g. siphonophores), which are capable of resonating at 38 kHz at depth (e.g. Kloser et al. 2016). These organisms are poorly sampled by nets because their fragile bodies fragment (Davison et al. 2015b). Species of calycophoran siphonophores (suborder Calycophorae, Order Siphonophora) which are characterised by loss of the gas-filled pneumatophore (organ to which resonance is attributed to), have been caught in some mid-water trawls in 2011 (research voyage TAN1116, siphonophores present in 6 trawls, with maximum contribution 0.8% in numbers), and in more recent research voyages (NIWA, unpublished data). Although never dominant in number or weight, squids were also often caught (see Escobar-Flores et al. 2018a). Squid are widely distributed in the epi-, meso- and bathypelagic zones of the SO, where the most abundant and broadly distributed species are *Galiteuthis glacialis* and some belonging to the family Bachioteuthidae (Collins and Rodhouse 2006). Squid are weak individual targets at 38 kHz, but may be detected if they form aggregations or dense layers (Goss et al. 2001).

Acoustic backscatter collected opportunistically can be used to study the distribution of MTL organisms in remote areas. However, to convert backscatter to density usually requires dedicated sampling to provide biological information to characterise species communities. Acoustic backscatter may not correlate with patterns of density of mesopelagic fish, and this needs to be taken into account when developing MTL predictive models that use acoustic data for parametrisation and validation. To advance our estimates, we need to carry out more *TS* experiments, if possible establish *TS*–*L* relationships for the dominant non-resonant species, obtain more accurate parameters for modelling *TS* of mesopelagic fish and improve our knowledge on mesopelagic fish swimbladder morphology and ontogenic changes. Though resonance can bias estimates of abundance of mesopelagic fish and hinder the linear conversion of acoustic backscatter collected at 38 kHz into densities of fish (Davison et al. 2015a;

Kloser et al. 2016; Proud et al. 2018), it does not affect all regions equally (it is species and size dependant), therefore, we need studies to shift from global to regional scales, to reach accurate global estimates of mesopelagic fish biomass.

Acknowledgements Funding for this study was provided by the Advanced Human Capital Programme, National Commission of Scientific and Technological Research (CONICYT, CHILE), through a Becas-Chile Doctorate scholarship, the National Institute of Water and Atmospheric Research (NIWA—New Zealand), through a NIWA Science Award Grant, and the New Zealand Ministry of Business, Innovation, and Employment (MBIE) through the Endeavour Fund Programme *Ross-RAMP*. Thanks to NIWA for providing the data and the facilities for undertaking this research, and to Dr Martin Cox for providing krill target strength estimates.

Compliance with ethical standards

Conflict of interest The authors declare that they have no conflict of interest.

Ethical approval All fish used in this research were collected by a mid-water research trawl under special permit for the New Zealand Ministry for Primary Industries. Special permits were granted under Section 97 of the Fisheries Act 1996 to authorize taking aquatic life for the purpose of investigative research. No fish were CITES listed.

References

- Azzali M, Leonori I, Biagiotti I et al (2010) Target strength studies on Antarctic Silverfish (*Pleuragramma antarcticum*) in the Ross Sea. *CCAMLR Sci* 17:75–104
- Bianchi D, Galbraith ED, Carozza DA et al (2013) Intensification of open-ocean oxygen depletion by vertically migrating animals. *Nat Geosci* 6:545–548. <https://doi.org/10.1038/ngeo1837>
- Brierley AS, Axelsen BE, Buecher E et al (2001) Acoustic observations of jellyfish in the Namibian Benguela. *Mar Ecol Prog Ser* 210:55–66. <https://doi.org/10.3354/meps210055>
- Brodeur R, Yamamura O (2005) Micronekton of the North Pacific. PICES Working Group 14 Final Report, Sydney
- Calise L, Skaret G (2011) Sensitivity investigation of the SDWBA Antarctic krill target strength model to fatness, material contrasts and orientation. *CCAMLR Sci* 18:97–122
- Catul V, Gauns M, Karuppasamy PK (2011) A review on mesopelagic fishes belonging to family Myctophidae. *Rev Fish Biol Fish* 21:339–354. <https://doi.org/10.1007/s11160-010-9176-4>
- Chindonova YG (1987) Quantitative information on the distribution of mesopelagic fish in the South Atlantic Ocean. In: Novikov NP, Alekseev AP (eds) Resources of the Southern Ocean and problems of their rational use. *YugNIRO, Kerch*, pp 113–114
- Coetzee J, Krakstad J-O, Stenevik EK et al (2006) Acoustic survey of the mesopelagic fish resources of the Benguela region. *Benefit Surveys RWG 2006-05*, Bergen
- Collins MA, Rodhouse PGK (2006) Southern Ocean Cephalopods. *Adv Mar Biol* 50:191–265. [https://doi.org/10.1016/S0065-2881\(05\)50003-8](https://doi.org/10.1016/S0065-2881(05)50003-8)
- Collins MA, Xavier JC, Johnston NM et al (2008) Patterns in the distribution of myctophid fish in the northern Scotia Sea ecosystem. *Polar Biol* 31:837–851. <https://doi.org/10.1007/s00300-008-0423-2>

- Collins MA, Stowasser G, Fielding S et al (2012) Latitudinal and bathymetric patterns in the distribution and abundance of mesopelagic fish in the Scotia Sea. *Deep Sea Res Part II Top Stud Oceanogr* 59–60:189–198. <https://doi.org/10.1016/j.dsr2.2011.07.003>
- Davison P (2011) The specific gravity of mesopelagic fish from the northeastern Pacific Ocean and its implications for acoustic backscatter. *ICES J Mar Sci* 68:2064–2074. <https://doi.org/10.1093/icesjms/fsr140>
- Davison PC, Koslow JA, Kloser RJ (2015a) Acoustic biomass estimation of mesopelagic fish: backscattering from individuals, populations, and communities. *ICES J Mar Sci* 72:1413–1424. <https://doi.org/10.1093/icesjms/fst048>
- Davison PC, Lara-Lopez A, Koslow JA (2015b) Mesopelagic fish biomass in the southern California current ecosystem. *Deep Sea Res Part II Top Stud Oceanogr* 112:129–142. <https://doi.org/10.1016/j.dsr2.2014.10.007>
- De Robertis A, Higginbottom I (2007) A post-processing technique to estimate the signal-to-noise ratio and remove echosounder background noise. *ICES J Mar Sci* 64:1282–1291
- Demer DA, Conti SG (2005) New target-strength model indicates more krill in the Southern Ocean. *ICES J Mar Sci* 62:25–32. <https://doi.org/10.1016/j.icesjms.2004.07.027>
- Demer DA, Berger L, Bernasconi M et al (2015) Calibration of acoustic instruments. ICES Cooperative Research Report No. 326, Copenhagen
- Donnelly J, Torres JJ, Sutton TT, Simoniello C (2004) Fishes of the eastern Ross Sea, Antarctica. *Polar Biol* 27:637–650. <https://doi.org/10.1007/s00300-004-0632-2>
- Dornan T, Fielding S, Saunders RA, Genner MJ (2019) Swimbladder morphology masks Southern Ocean mesopelagic fish biomass. *Proc R Soc B Biol Sci* 286:20190353. <https://doi.org/10.1098/rspb.2019.0353>
- Echoview Software Pty Ltd (2013) Echoview software, version 5.4. Echoview Software Pty Ltd, Hobart
- Edwards JL, Armstrong F, Magurran AE, Pitcher TJ (1984) Herring, mackerel and sprat target strength experiments with behavioural observations. ICES Fish Capture Committee
- Efron B, Tibshirani RJ (1993) An introduction to the bootstrap. Chapman & Hall, New York
- Escobar-Flores PC (2017) The use of acoustics to characterise mid-trophic levels of the Southern Ocean pelagic ecosystem. PhD thesis. University of Auckland
- Escobar-Flores P, O'Driscoll RL, Montgomery JC (2013) Acoustic characterization of pelagic fish distribution across the South Pacific Ocean. *Mar Ecol Prog Ser* 490:169–183. <https://doi.org/10.3354/meps10435>
- Escobar-Flores PC, O'Driscoll RL, Montgomery JC (2018a) Spatial and temporal distribution patterns of acoustic backscatter in the New Zealand sector of the Southern Ocean. *Mar Ecol Prog Ser* 592:19–35
- Escobar-Flores PC, O'Driscoll RL, Montgomery JC (2018b) Predicting distribution and relative abundance of mid-trophic level organisms using oceanographic parameters and acoustic backscatter. *Mar Ecol Prog Ser* 592:37–56
- Filin AA, Gorchinsky KV, Kiseleva VM (1990) Biomass of myctophids in the atlantic sector of the SO as estimated by acoustic surveys. CCAMLR Sel Sci Pap WG-FSA-90:417–431
- Flynn AJ, Williams A (2012) Lanternfish (Pisces: Myctophidae) biomass distribution and oceanographic—topographic associations at Macquarie Island, Southern Ocean. *Mar Freshw Res* 63:251–263. <https://doi.org/10.1071/MF11163>
- Foote G (1980) Importance of the swimbladder in acoustic scattering by fish: A comparison of gadoid and mackerel target strengths. *J Acoust Soc Am* 67:2084–2089
- Foote KG, Aglen A, Nakken O (1986) Measurement of fish target strength with a split-beam echo sounder. *J Acoust Soc Am* 80:612–621. <https://doi.org/10.1121/1.394056>
- Fujino T, Sadayasu K, Abe K et al (2009) Swimbladder morphology and target strength of a mesopelagic fish, *Maurollicus japonicus*. *J Mar Acoust Soc Jpn* 36:241–249. <https://doi.org/10.3135/jmasj.36.241>
- Gauthier S, Oeffner J, O'Driscoll RL (2014) Species composition and acoustic signatures of mesopelagic organisms in a subtropical convergence zone, the New Zealand Chatham Rise. *Mar Ecol Prog Ser* 503:23–40. <https://doi.org/10.3354/meps10731>
- Gjøsaeter J, Kawaguchi K (1980) A review of the world resources of mesopelagic fish. FAO Fisheries Technical Paper 193
- Goss C, Middleton D, Rodhouse P (2001) Investigations of squid stocks using acoustic survey methods. *Fish Res* 54:111–121. [https://doi.org/10.1016/S0165-7836\(01\)00375-7](https://doi.org/10.1016/S0165-7836(01)00375-7)
- Greene CH, Stanton TK, Wiebe PH, McClatchie S (1991) Acoustic estimates of Antarctic krill. *Nature* 349:110
- Handegard NO, Buisson L, Brehmer P et al (2013) Towards an acoustic-based coupled observation and modelling system for monitoring and predicting ecosystem dynamics of the open ocean. *Fish Fish* 14:605–615. <https://doi.org/10.1111/j.1467-2979.2012.00480.x>
- Heino M, Porteiro FM, Sutton TT et al (2011) Catchability of pelagic trawls for sampling deep-living nekton in the mid-North Atlantic. *ICES J Mar Sci* 68:377–389. <https://doi.org/10.1093/icesjms/fsq089>
- Hulley PA (1990) Family Myctophidae. In: Gon O, Heemstra PC (eds) *Fishes of the Southern Ocean*. J.L.B Smith Institute of Ichthyology, Grahamstown, pp 146–178
- Irigoien X, Klevjer TA, Røstad A et al (2014) Large mesopelagic fishes biomass and trophic efficiency in the open ocean. *Nat Commun* 5:3271. <https://doi.org/10.1038/ncomms4271>
- Kaartvedt S, Staby A, Aksnes DL (2012) Efficient trawl avoidance by mesopelagic fishes causes large underestimation of their biomass. *Mar Ecol Prog Ser* 456:1–6. <https://doi.org/10.3354/meps09785>
- Kloser RJ, Ryan T, Sakov P et al (2002) Species identification in deep water using multiple acoustic frequencies. *Can J Fish Aquat Sci* 59:1065–1077. <https://doi.org/10.1139/f02-076>
- Kloser RJ, Ryan TE, Young JW, Lewis ME (2009) Acoustic observations of micronekton fish on the scale of an ocean basin: potential and challenges. *ICES J Mar Sci* 66:998–1006. <https://doi.org/10.1093/icesjms/fsp077>
- Kloser RJ, Ryan TE, Keith G, Gershwin L (2016) Deep-scattering layer, gas-bladder density, and size estimates using a two-frequency acoustic and optical probe. *ICES J Mar Sci* 73:2037–2048. <https://doi.org/10.1093/icesjms/fst034>
- Kozlov AN, Shust K V, Zemsky A V (1990) Seasonal and inter-annual variability in the distribution of *Electrona carlsbergi* in the Southern Polar Front area (the area to the north of South Georgia is used as an example). CCAMLR Sel Sci Pap WG-FSA-90:337–368
- La HS, Lee H, Kang D et al (2015) Ex situ echo sounder target strengths of ice krill *Euphausia crystallorophias*. *Chin J Oceanol Limnol* 33:802–808
- Lancraft TM, Torres JJ, Hopkins TL (1989) Micronekton and Macrozooplankton in the Open waters near Antarctic ice edge zones (AMERIEZ 1983 and 1986). *Polar Biol* 9:225–233
- Lehodey P, Murtugudde R, Senina I (2010) Bridging the gap from ocean models to population dynamics of large marine predators: a model of mid-trophic functional groups. *Prog Oceanogr* 84:69–84. <https://doi.org/10.1016/j.pocean.2009.09.008>
- Lehodey P, Conchon A, Senina I et al (2015) Optimization of a micronekton model with acoustic data. *ICES J Mar Sci* 72:1399–1412. <https://doi.org/10.1093/icesjms/fsu233>
- Love RH (1978) Resonant acoustic scattering by swimbladder-bearing fish. *J Acoust Soc Am* 64:571. <https://doi.org/10.1121/1.382009>

- Macaulay G, Hart A, Grimes P et al (2002) Estimation of the target strength of Oreo and associated species. Final Research Report for Ministry of Fisheries Research Project OE02000/01A. National Institute of Water and Atmospheric Research, Wellington
- Marshall NB (1960) Swimbladder structure of deep-sea fishes in relation to their systematics and biology. Cambridge University Press, Cambridge
- McClatchie S, Dunford A (2003) Estimated biomass of vertically migrating mesopelagic fish off New Zealand. Deep Sea Res Part I Oceanogr Res Pap 50:1263–1281. [https://doi.org/10.1016/S0967-0637\(03\)00128-6](https://doi.org/10.1016/S0967-0637(03)00128-6)
- McGinnis RF (1982) Biogeography of the lanternfishes (Myctophidae) south of 30°S. American Geophysical Union, Washington DC
- Ménard F, Marchal E (2003) Foraging behaviour of tuna feeding on small schooling *Vinciguerria nimbaria* in the surface layer of the equatorial Atlantic Ocean. Aquat Living Resour 16:231–238. [https://doi.org/10.1016/S0990-7440\(03\)00040-8](https://doi.org/10.1016/S0990-7440(03)00040-8)
- Nelson JS (2006) Fishes of the World, 4th edn. Wiley, Fourth
- O'Driscoll RL (2004) Estimating uncertainty associated with acoustic surveys of spawning hoki (*Macruronus novaezelandiae*) in Cook Strait, New Zealand. ICES J Mar Sci 61:84–97. <https://doi.org/10.1016/j.icesjms.2003.09.003>
- O'Driscoll RL, Macaulay GJ, Gauthier S et al (2011) Distribution, abundance and acoustic properties of Antarctic silverfish (*Pleuragramma antarcticum*) in the Ross Sea. Deep Sea Res Part II Top Stud Oceanogr 58:181–195. <https://doi.org/10.1016/j.dsr2.2010.05.018>
- Proud R, Handegard NO, Kloser RJ et al (2018) From siphonophores to deep scattering layers: uncertainty ranges for the estimation of global mesopelagic fish biomass. ICES J Mar Sci. <https://doi.org/10.1093/icesjms/fsy037>
- Robertson DA, Roberts PE, Wilson JB (1978) Mesopelagic faunal transition across the subtropical convergence east of New Zealand. New Zeal J Mar Freshw Res 12:295–312. <https://doi.org/10.1080/00288330.1978.9515757>
- Rose G (1998) Acoustic target strength of capelin in Newfoundland waters. ICES J Mar Sci 55:918–923. <https://doi.org/10.1006/jmsc.1998.0358>
- Rose G, Gauthier S, Lawson G (2000) Acoustic surveys in the full Monte: simulating uncertainty. Aquat Living Resour 13:367–372. [https://doi.org/10.1016/S0990-7440\(00\)01074-3](https://doi.org/10.1016/S0990-7440(00)01074-3)
- Ryan TE, Downie RA, Kloser RJ, Keith G (2015) Reducing bias due to noise and attenuation in open-ocean echo integration data. ICES J Mar Sci J Cons 72:2482–2493. <https://doi.org/10.1093/icesjms/fsv121>
- Sawada K, Uchikawa K, Matsuura T et al (2011) In situ and ex situ target strength measurement of mesopelagic lanternfish, diaphus theta (family myctophidae). J Mar Sci Technol 19:302–311
- Scouling B, Chu D, Ona E, Fernandes PG (2015) Target strengths of two abundant mesopelagic fish species. J Acoust Soc Am 137:989–1000. <https://doi.org/10.1121/1.4906177>
- Simmonds J, MacLennan DN (2005) Fisheries acoustics: theory and practice, 2nd edn. Wiley-Blackwell, Oxford
- Stanton TK (1988) Sound scattering by cylinders of finite length. I. Fluid cylinders. J Acoust Soc Am 83:55–63
- Wiebe PH, Chu D, Kaartvedt S et al (2010) The acoustic properties of *Salpa thompsoni*. ICES J Mar Sci 67:583–593. <https://doi.org/10.1093/icesjms/fsp263>
- Yasuma H, Sawada K, Ohshima T et al (2003) Target strength of mesopelagic lanternfishes (family Myctophidae) based on swimbladder morphology. ICES J Mar Sci 60:584–591. <https://doi.org/10.1016/S1054>
- Yasuma H, Takao Y, Sawada K et al (2006) Target strength of the lanternfish, *Stenobrachius leucopsarus* (family Myctophidae), a fish without an airbladder, measured in the Bering Sea. ICES J Mar Sci 63:683–692. <https://doi.org/10.1016/j.icesjms.2005.02.016>
- Yasuma H, Sawada K, Takao Y et al (2010) Swimbladder condition and target strength of myctophid fish in the temperate zone of the Northwest Pacific. ICES J Mar Sci 67:135–144. <https://doi.org/10.1093/icesjms/fsp218>
- Ye Z (1997) Low-frequency acoustic scattering by gas-filled prolate. J Acoust Soc Am 101:1945–1952

Publisher's Note Springer Nature remains neutral with regard to jurisdictional claims in published maps and institutional affiliations.